JACS
JOURNAL OF THE AMERICAN CHEMICAL SOCIETY

Article

pubs.acs.org/JACS

Gemcitabine–Coumarin–Biotin Conjugates: A Target Specific Theranostic Anticancer Prodrug

Sukhendu Maiti,[†] Nayoung Park,[†] Ji Hye Han,[‡] Hyun Mi Jeon,[‡] Jae Hong Lee,[†] Sankarprasad Bhuniya,[†] Chulhun Kang,*[,‡] and Jong Seung Kim*[,†]

[†]Department of Chemistry, Korea University, Seoul, 136-701, Korea

[‡]The School of East-West Medical Science, Kyung Hee University, Yongin, 446-701, Korea

Supporting Information

ABSTRACT: We present here, the design, synthesis, spectroscopic characterization, and *in vitro* biological assessment of a gemcitabine–coumarin–biotin conjugate (**5**). Probe **5** is a multifunctional molecule composed of a thiol-specific cleavable disulfide bond, a coumarin moiety as a fluorescent reporter, gemcitabine (GMC) as a model active drug, and biotin as a cancer-targeting unit. Upon addition of free thiols that are relatively abundant in tumor cells, disulfide bond cleavage occurs as well as active drug GMC release and concomitantly fluorescence intensity increases. Confocal microscopic experiments reveal that **5** is preferentially taken up by A549 cells rather than WI38 cells. Fluorescence-based colocalization studies using lysosome- and endoplasmic reticulum-selective dyes suggest that thiol-induced disulfide cleavage of **5** occur in the lysosome possibly via receptor-mediated endocytosis. The present drug delivery system is a new theranostic agent, wherein both a therapeutic effect and drug uptake can be readily monitored at the subcellular level by two photon fluorescence imaging.

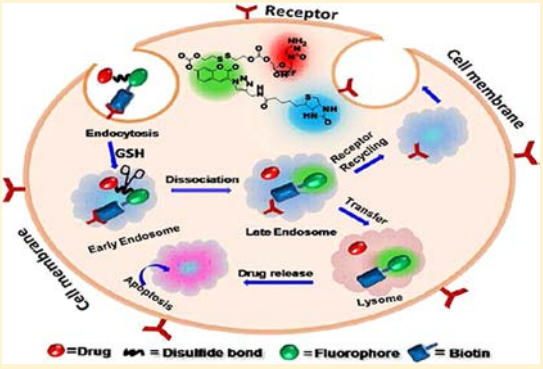

1. INTRODUCTION

Target-specific drug delivery, frequently called smart drug delivery system (DDS), is an important and exciting as well as challenging area in our science community and in modern pharmaceutical industry.[1] Its presumed advantages are the reduction in the frequency of the dosages taken by the patient and reduced fluctuation in circulating drug levels and drug side effects. This method is able to provide information regarding real-time monitoring of the release and distribution of a drug.[2] Therefore, *in situ* monitoring of the active drug release in DDSs could be of great benefit, particularly if the reported signal could be detected in a noninvasive manner. On the other hand, imaging the molecular expressions of disease may help early detection, thus facilitating more effective early therapy or change in lifestyle. This approach may also help in characterizing different plaques for the purpose of treatment guidance as well as assessing the response to therapy.

The variable forms of drug carriers are widely used in the targeted DDS system, such as gold nanoparticles,[3] fluorescent quantum dots,[4] polymeric materials,[5] and porous silica materials.[6] However, these methods suffer from extensive and time-consuming procedures to visualize the targets concerned. Recently, a theranostic (therapy and diagnostics) DDS equipped with targeting and reporting abilities was introduced by our group, where the target-specific cellular uptake of a RGD peptide-appended therapeutic agent conjugated with camptothecin, and the drug release was monitored based upon fluorescence.[7]

Gemcitabine (GMC) is a nucleoside analogue used for an antimetabolite of deoxycytidine[8] to control nonsmall cell lung,[9] pancreatic,[10] metastatic breast, and recurrent ovarian cancers.[11] Despite the clinical success of GMC, its short plasma half-life (9–13 min for human plasma)[12] and adverse toxicity, such as myelosuppression, greatly limit its chemotherapeutic efficacy. To increase its chemotherapeutic index, it would be desirable to develop a new strategy, for example, attachment of a disulfide linker on the GMC molecule to protect the drug from renal clearance and prolonged circulation half-life.[13] Besides, it is hard to monitor the delivery of such a drug *in vitro* and *in vivo*, since GMC is a nonfluorescent antitumor agent. For these reasons, it would be a significant advance in GMC delivery to develop a new type of GMC conjugate which is able to real-time monitor the drug delivery and to enhance its lifetime in circulation at the same time. Therefore, in view of demand, we wish to design, synthesize, and spectroscopically characterize a GMC delivery system in a specific region as well as fluorescence-on, for in *vivo* and *vitro* use.

Herein, we develop a cancer-targeting theranostic DDS that contains a GMC-loaded coumarin moiety which is coupled with biotin as a targeting ligand. It is known that biotin molecules or biotin conjugates can be taken up preferentially by a cancer cell.[14] Conjugate **5** is composed of the chemotherapeutic drug GMC, a disulfide linker cleavable by the

Received: February 5, 2013
Published: March 5, 2013

dx.doi.org/10.1021/ja401350x | *J. Am. Chem. Soc.* 2013, 135, 4567–4572

intracellular thiols, a coumarin moiety, which enhances the fluorescence intensity after disulfide bond cleavage, and biotin, which serves as an excellent guiding molecule to tumor cells.

2. RESULTS AND DISCUSSION

Synthesis of compound **5** was performed according to the following synthetic route shown in Scheme 1. The coumarin−

Scheme 1. Synthetic Routes of 5 and 9

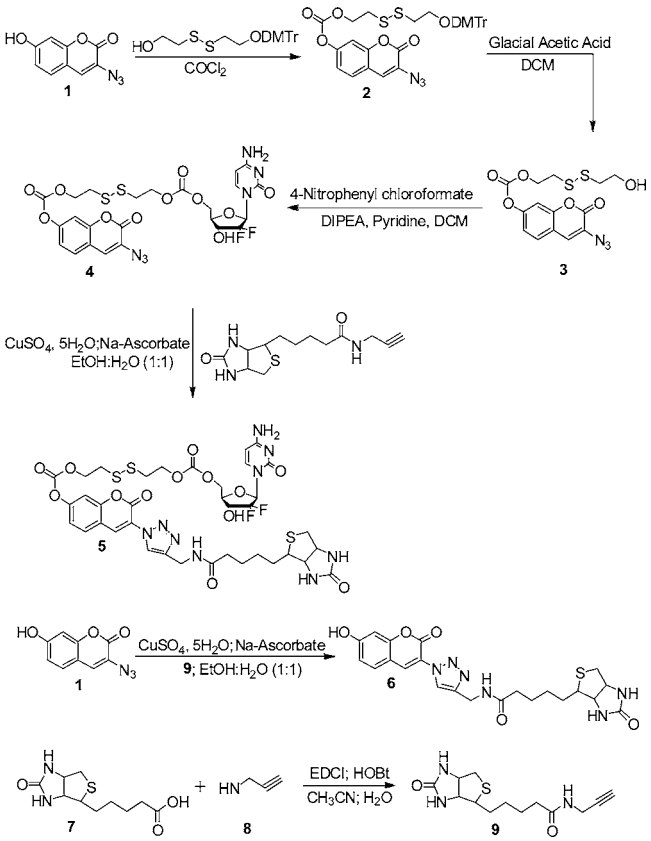

disulfide conjugates **1**−**3** were synthesized by previously reported methods.[15,7] The compound **3** was reacted with 4-nitrophenyl chloroformate and diisopropylethylamine (DIPEA) and followed by reaction with GMC to afford **4** in moderate yield. Then, the target **5** was prepared by the Click reaction of **4** with a biotin derivative in moderate yield. The coumarin derivative **6** as the reference compound and the biotin derivative **9** were prepared from the previously reported procedures.[15,16] The identities of all compounds (**1**−**6**) were confirmed by ^{1}H NMR, ^{13}C NMR, ESI-MS, and HRMS data (Supporting Information, SI).

To demonstrate whether the disulfide bond between the coumarin and the GMC moieties of compound **5** is cleavable or not by biologically available thiols, **5** was allowed to react with 0−60 equiv of glutathione (GSH), and the changes in its absorption and fluorescence spectra were monitored. In the UV spectrum, as seen in Figure 1a, **5** exhibited a strong absorption band at λ_{max} 400 nm, whose intensity increases by ∼3-fold upon addition of GSH. Although the solution of **5** exhibited weak fluorescence centered at 476 nm on excitation at 410 nm, upon addition of 5.0 mM GSH, its intensity was 3.5-fold enhanced, as revealed in Figure 1b. The emission spectrum of the solution was identical with that of the reference **6** (Figure S1). On

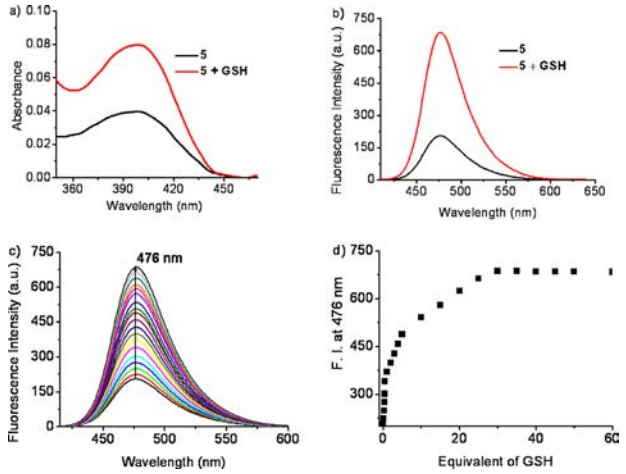

Figure 1. (a) Absorption spectra of **5** (25.0 μM, 25% DMSO, and 75% PBS buffer) recorded in the presence and absence of GSH (5.0 mM). (b) Fluorescence spectra of **5** (5.0 μM) recorded in the presence and absence of GSH (5.0 mM). (c) Fluorescence changes of **5** (5.0 μM) seen upon treatment with increasing concentrations of GSH (0−60 equiv). (d) Changes in fluorescence intensity at 476 nm as a function of GSH concentration.

stepwise addition of GSH to the solution of probe **5** (5.0 μM) in aqueous PBS buffer, the solution's fluorescence intensity at λ_{max} 476 nm gradually increased with each additional step up to 0−30 equiv of GSH (Figure 1c,d). These results indicate that the disulfide bond of **5** can be readily cleavable by GSH, the most abundant thiol in cells, in a dose-dependent manner, possibly to release GMC in cells.

Whether the cleavage reaction of probe **5** is interfered by the biological environments, such as various biochemical species or pH, should be an important question to be answered prior to its application to the biosystems. For the possibility of the interference from other biologically relevant analytes, the reactions of **5** with different thiols, nonthiol amino acids, and metal ions were examined. Upon the addition of cysteine (Cys) or homocysteine (Hcy) to probe **5**, similar spectroscopic changes were observed to that of GSH. In contrast, addition of any nonthiol amino acids or biologically relevant metal ions to the solution containing **5**, no significant spectroscopic changes were observed (Figure S2). These results indicate that the fluorescence enhancement from the cleavage reaction of the disulfide in **5** is induced by the thiol species. Furthermore, we have also investigated the pH dependency studies where the fluorescence intensity changes of **5** (5.0 μM), with the addition of 5.0 mM GSH under different pH conditions. The large fluorescence enhancement at λ_{em} 476 nm was observed over a pH range of 6−9 (Figure S3). Therefore, at this stage we can conclude that the disulfide-linked GMC−coumarin conjugates will undergo thiol-mediated cleavage with no significant interference from other biomolecules, such as amino acids or metal cations, even in biological environments.

It is quite intersting to ask whether the fluorescence enhancement from **5** in Figure 1 means GMC release or not. To answer the question, the temporal release of GMC from **5** and the fluorescence changes in a function of time was measured in the presence of GSH as shown in Figures S4 and S23. In Figure S4, it is observed that, within 10 min, the enhancement of fluorescence intensity of **5** reached the saturation point, implicating that it mostly dissociated. We observed that for 5.0 mmol GSH, the reaction rate is higher

dx.doi.org/10.1021/ja401350x | J. Am. Chem. Soc. 2013, 135, 4567−4572

than that of 1.0 and 3.0 mmol GSH. In contrast, in the absence of GSH, monitoring solutions of **5** revealed neither GMC release nor an enhancement in the fluorescence intensity at 476 nm as a function of time. Furthermore, probe **5** was treated with 5.0 mmol GSH at 37 °C for 1 h, the aliquot was subjected to mass analysis, and the solutions gave rise to two major peaks associated with GMC ([M+H] = 264.2) and **6** ([M+H] = 485.3) (Figure S23). The above results lead us to confirm that active GMC was released after the disulfide bond cleavage upon GSH treatment.

Together, these results suggest that, by the action of GSH, the vulnerable S−S bond cleaved and the resulting thiol undergoes an intramolecular nucleophilic substitution at the carabamate moiety, forming a five-membered ring thiolactone and releasing GMC molecules in a pharmaceutically active form, consequently inducing the fluorescence enhancement of the product **6**, which is summarized in Scheme 2. This type of self-immolative disulfide linker can readily be applied to a variety of tumor-targeting drug conjugates.

Scheme 2. Reaction Mechanism of 5 with GSH under Physiological Conditions

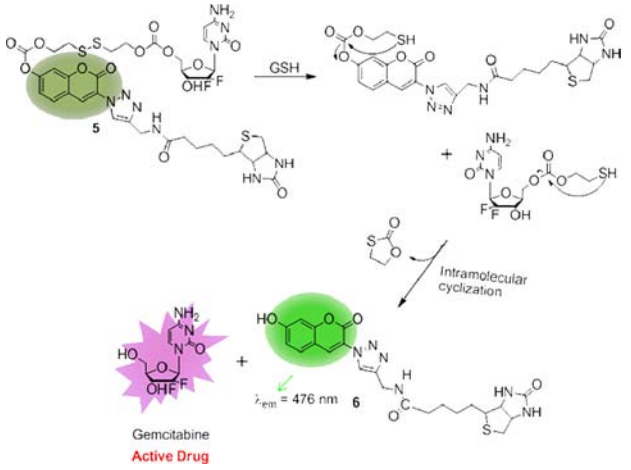

Based upon the results summarized in Scheme 2, it is worth examining whether DDS works in live cells similarly or not. The encouraging response toward thiol-mediated active drug recovery and concomitantly optical enhancement *in vitro* solution test of theranostic prodrug **5** is committed to apply in living cells. Apparently, the optical response of **6**, using one-photon fluorescent spectroscopy, is not worthy to use in living systems, as the shorter wavelength light scattered and auto absorbed by native cellular components. Therefore, we adopted the two-photon fluorescent spectroscopy tool for cellular imaging. It is fortuitous that the coumarin moiety in **6** showed a two-photon absorption property.[17] This tool reduced photodamage to living biological samples and fluorophore, minimized background absorption and scattering, and improved the spatial resolution and sensitivity and the ability to image thicker specimens.

For the application of probe **5** to the biological systems, we investigated whether the biotin moiety can guide the probe preferentially to biotin receptor-positive or biotin receptor-negative tumor cells. Probe **5** was incubated with A549 and WI38 cells, which are known to be biotin receptor-positive and -negative cells, respectively. As shown in Figure 2, the A549 cells demonstrate strong fluorescence intensity within a 15 min

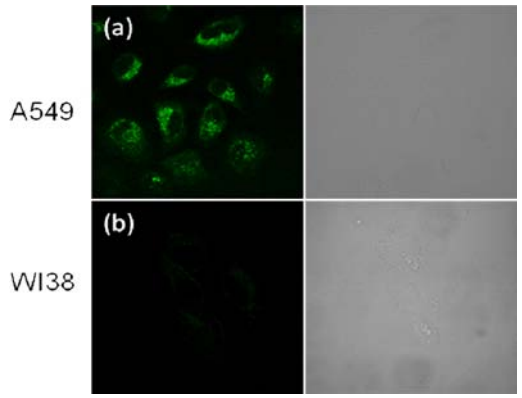

Figure 2. Confocal microscopy images of A549 and WI38 cells treated with **5.** The left-side panels show the confocal microscopy images of A549 and WI38 cells treated with 10.0 μM of 5 in PBS buffer and a total incubation period of 15 min. The right-side panels show nonconfocal phase contrast images. Cell images were obtained using two photon excitation at 750 nm and a long-path (420−600 nm) emission filter.

incubation of compound **5**, whereas the WI38 cells show little or no fluorescence signal under a similar experimental condition. The result confirms that the presence of biotin receptor only on the A549 cells causes the difference in the fluorescence intensity for two cell lines. The difference might be possible if the concentration of thiol species (for example, GSH) is much lower in WI38 cells, however, it seems unreasonable since GSH is essential to all types of eukaryotic cells including both cell lines in this experiment. Therefore, we conclude that the prodrug **5** can enter the cells, aided by the interaction of its biotin moiety with a biotin receptor on the tumor cells, possibly through receptor-mediated endosytosis.

To provide further evidence for thiol-induced disulfide bond cleavage as well as concomitantly fluorescence-on, the probe **5** was studied in the presence of a strong thiol reacting agent, *N*-ethylmalemide (NEM).[18] The results obtained from these studies are shown in Figure 3. We found that the fluorescence

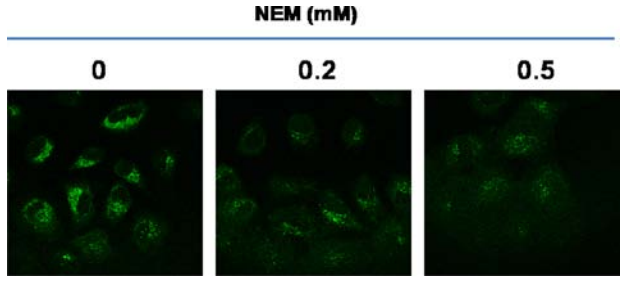

Figure 3. Confocal microscopy images of A549 cells treated with **5**. The cells were preincubated with media containing NEM of various concentrations (0, 0.2, and 0.5 mM) for 30 min at 37 °C. Cell images were obtained using two photon excitation wavelengths of 750 nm and emission wavelengths of 525−600 nm, green signal, respectively.

intensity of **5** in A549 cells decreases as the concentration of NEM is increased (0−0.5 mM). This observed result indicates that fluorescence come from compound **6** generated by the S−S bond cleavage of probe **5** by intracellular thiols.

To identify the intracellular location of GMC release from **5**, after entering the cells, colocalization experiments were performed using fluorescent endoplasmic reticulum (ER)- and lysosome-selective markers. As seen in the panels of

dx.doi.org/10.1021/ja401350x | J. Am. Chem. Soc. 2013, 135, 4567−4572

Figure 4, the fluorescence ascribable to **5** colocalizes well with lyso tracker (panel 1) but does not exactly match what is

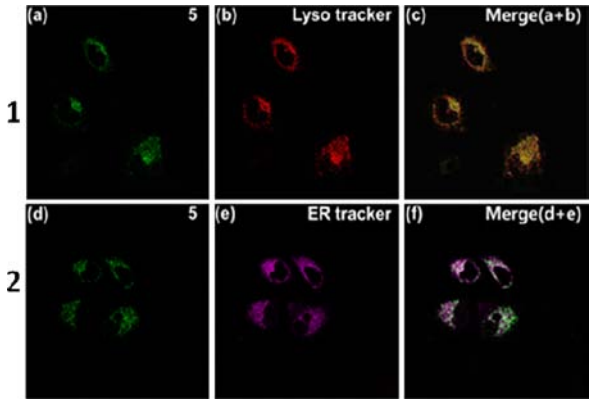

Figure 4. Confocal microscopic images of colocalized experiment in A549 cells. (a,d) Flourescence images of A549 cells contained with **5** (10.0 μM) for 25 min. (b) Flourescence image of A549 cells incubated with **5** (10.0 μmol) as well as lyso tracker blue DND-167 (0.05 μM) for 25 min. (c) Overlay of the merged images of (a) and (b). (e) Flourescence image of A549 cells incubated with **5** (10.0 μM) and ER tracker red (0.05 μM) for 25 min. (f) Overlay of the merged images of (d) and (e). Images of the cells were obtained using excitation wavelengths of 750 nm, a band path (350−440 nm, blue signal), (550−600 nm, green signal), and (650−690 nm, red signal), and emission filters, respectively.

observed in the case of ER tracker (panel 2). Therefore, it is noteworthy that thiol-induced disulfide cleavage of **5** occurs in the lysosome, serving to release the GMC molecule, which presumably diffuses into the cell nucleus where it replaces one of the building blocks of nucleic acids, cytidine, during DNA replication. This process leads to form a faulty nucleoside, resulting in cell apoptosis.[19]

Finally, we investigated the anticancer effects of probes **5** bearing biotin moiety and **4** without biotin to demonstrate the targeting unit effect for cancer cells. Comparison of the cell viabilities of **5** with **4** toward A549 cells as well as toward WI38 cells was conducted where they are positive and negative regarding biotin accumulation ability, respectively.[14,20] We found that for A549 cells, compound **5** is a more potent anticancer drug than **4**, which is mostly evident in comparison of the cell viabilities at 1.0 μM of each compound (Figure 5). However, in a parallel experiment for WI38 cell lines, two probes fail to demonstrate such differences in cell viability at

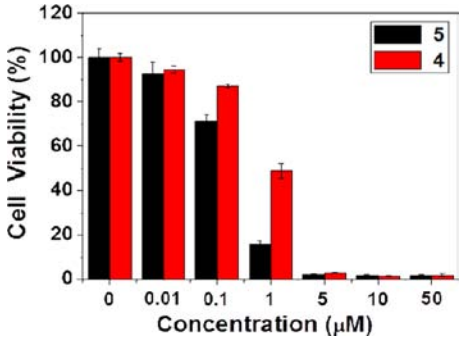

Figure 5. Cell viability of **5** and **4** on A549 cell lines. All compounds were incubated with the cells for 72 h, and the cell viability observed via MTT assay.

most concentrations of the probes (Figure S24). From these results, it is clearly confirmed again that the biotin moiety in **5** obviously plays as a targeting unit to tumor cells in this DDS.

3. CONCLUSIONS

In conclusion, we have reported a new theranostic agent, GMC−coumarin−biotin conjugate (**5**) and its synthesis, characterization, spectroscopic properties, and anticancer effects as well as biological applications. Upon addition of free thiol to compound **5**, the disulfide bond cleaved, followed by an intramolecular nucleophilic substitution at the carbamate moiety, forming a five-membered thiolactone ring. This leads to release of active GMC and also gives rise to fluorescence enhancement. The colocalization experiments using commercial available lysosome- as well as ER-selective dyes demonstrated that compound **5** localized to the lysosme after receptor-mediated endocytosis. According to confocal microscopic experimental studies, our final prodrug only goes to biotin receptor-positive A549 tumor cells, over biotin receptor-negative WI38 cells. Therefore, our DDS could provide a powerful new strategy for the specific tumor targeting drug delivery and cellular imaging.

4. EXPERIMENTAL SECTION

Synthesis of 1. This compound was synthesized, followed by reported procedure,[15] with the yield: 50%; ^{1}H NMR (DMSO-d_6, 400 MHz): δ 6.72 (d, J = 2.2 Hz, 1H), 6.77 (d, J = 2.3, 8.5 Hz, 1H), 7.44 (d, J = 8.6 Hz, 1H), 7.55 (s, 1H), 10.53 (s, phenolic OH), ppm. ^{13}C NMR (DMSO-d_6, 100 MHz): 102.7, 112.0, 114.5, 121.8, 128.5, 129.8, 153.4, 158.0, 161.0 ppm. HRMS: calcd for $C_9H_6O_3N_3$ (M+1), 204.0409; found, 204.0409.

Synthesis of 2. To a stirred solution of DMTr-protected hydroxyl ethyl disulfide (500 mg, 1.10 mmol) and DIPEA (849 mg, 6.57 mmol) in dry dichloromethane (DCM) (5.0 mL), a phosgene solution (429 mg, 4.38 mmol, 2.14 mL) was added. The reaction mixture was stirred at 0 °C under argon atmosphere. After 2 h, the excess phosgene was removed from the reaction mixture by argon purge. Then 3-azido-7-hydroxy coumarin (111 mg, 0.55 mmol) in dry DCM was added in the reaction mixture and was stirred overnight. After completion of the reaction (by TLC), the reaction mixture was diluted with EtOAc, washed twice with brine, dried over sodium sulfate, and then filtered, and the solvent was removed under reduced pressure. The crude product was purified by column chromatography on silica gel (EtOAc:hexanes 1:9 to 3:7) to give **2** (460 mg, 61% yield) as a yellow sticky liquid. ^{1}H NMR ($CDCl_3$, 400 MHz): δ 2.85−2.91 (m, 4H), 3.39 (t, J = 6.1 Hz, 2H), 3.77 (s, 6H), 4.46 (t, J = 6.6 Hz, 2H), 6.82 (d, J = 8.8 Hz, 4H), 7.11 (dd, J = 2.2, 8.5 Hz, 1H), 7.16−7.22 (m, 3H), 7.28 (t, J = 7.8 Hz, 2H), 7.34 (d, J = 8.8 Hz, 4H), 7.38 (d, J = 8.6 Hz, 1H), 7.45 (d, J = 7.3 Hz, 2H), ppm. ^{13}C NMR ($CDCl_3$, 100 MHz): 36.8, 39.9, 55.5, 62.0 67.1, 86.6, 109.8, 113.3, 113.3, 117.5, 118.6, 125.3, 126.3, 127.1, 128.1, 128.2, 128.4, 130.3, 136.2, 145.0, 151.8, 152.2, 152.9, 157.3, 158.7 ppm. ESI-MS: calcd for $C_{35}H_{32}N_3O_8S_2$, 685.16; found, 685.48.

Synthesis of 3. Compound **2** (450 mg, 0.65 mmol) was dissolved in 5.0 mL DCM solvent, and 80% glacial acetic acid was slowly added. The reaction mixture was kept for 24 h stirring to completion by TLC (EtOAc:hexanes 1:1). Glacial acetic acid was neutralized by the saturated aqueous sodium bicarbonate solution. EtOAc was added, the organic phase was dried over sodium sulfate and then filtered, and the solvent was removed under reduced pressure. The crude product was purified by column chromatography on silica gel (EtOAc:hexanes 2:8 to 5:5) to give **3** (180 mg, 71% yield) as a yellow sticky liquid. ^{1}H NMR ($CDCl_3$, 400 MHz): δ 2.87 (t, J = 5.8 Hz, 2H), 3.00 (t, J = 6.6 Hz, 2H), 3.86 (t, J = 5.8 Hz, 2H), 4.51 (t, J = 6.6 Hz, 2H), 7.11 (dd, J = 2.2, 8.6 Hz, 1H), 7.17−7.20 (m, 2H), 7.40 (d, J = 8.6 Hz, 1H), ppm. ^{13}C NMR ($CDCl_3$, 100 MHz): 36.7, 41.7, 60.5, 67.0, 109.8, 117.5,

dx.doi.org/10.1021/ja401350x | J. Am. Chem. Soc. 2013, 135, 4567−4572

118.6, 125.4, 126.3, 128.3, 151.7, 152.1, 152.9, 157.3 ppm. HRMS: calcd for $C_{14}H_{14}N_3O_6S_2$ (M+1), 384.0324; found, 384.0326.

Synthesis of 4. To a DCM (5 mL) solution of **3** (100 mg, 0.26 mmol) 4-nitrophenyl chloroformate (157.7 mg, 0.78 mmol), DIPEA (134 mg, 1.04 mmol) and a catalytic amount of pyridine were added at 0 °C and stirred for 5h at rt. Then the reaction mixture was concentrated *in vacuo*. The crude residue was dissolve in 5 mL DMF. To this solution, GMC (205 mg, 0.78 mmol) in DMF (2 mL) and TEA (0.5 mL) were added and continued to stir for 24 h. After completion of reaction, the reaction mixture was diluted in water. The compound was extracted with EA. The organic layer was dried over anhydrous sodium sulfate. The crude compound was passed through silica column chromatography using DCM/MeOH (9:1) as eluent to afford a sticky yellow liquid compound **4** (30 mg, 17% yield). ^{1}H NMR ($CDCl_3$, 400 MHz): δ 2.95−3.06 (m, 4H), 3.78 (s, 2H), 3.99−4.14 (m, 2H), 4.66−4.55 (m, 4H), 5.30 (s, 1H), 5.82(d, J = 6.00 Hz, 1H), 6.23(br s, 1H), 7.14 (d, J = 6.5 Hz, 1H), 7.22−7.23 (m, 1H), 7.37−7.45 (m, 2H), 7.55 (br s, 1H), 8.26 (d, J = 7.2 Hz, 1H), ppm. ^{13}C NMR ($CDCl_3$, 100 MHz): 36.6, 36.9, 55.1, 59.7, 65.6, 66.9, 79.0, 95.9, 109.6, 117.4, 118.5, 121.9, 125.5, 125.4, 128.2, 141.6, 151.6, 152.8, 153.8, 155.6, 156.0, 165.9, 166.1 ppm. HRMS: calcd for $C_{24}H_{23}F_2N_6O_{11}S_2$ (M+1), 673.0834; found, 673.0833.

Synthesis of 5. To a MeOH (3.0 mL) solution of **4** (70 mg, 0.01 mmol), **9** (29 mg, 0.01 mmol) and sodium ascorbate (10 mol %) were added. The reaction mixture as degassed for 15 min by purging argon gas. Then 2 mg (0.002 mmol) of $CuSO_4$ in 0.5 mL water was added to the reaction mixture and stirred for an additional 3 h. The crude reaction mixture was directly passed through silica column chromatography using DCM/MeOH (8.5:1.5) as eluent to afford a yellow sticky liquid compound **5** (25 mg, 25% yield). ^{1}H NMR (300 MHz, DMSO-d_6): δ 1.21−1.32 (m, 2H), 1.36−1.58 (m, 4H), 2.05 (t, J = 7.3 Hz, 2H), 2.53−2.57 (m, 2H), 2.77−2.83 (m, 2H), 2.99−3.10 (m, 5H), 3.68 (br s, 2H), 3.79−3.82 (m, 3H), 4.08−4.12 (m, 2H), 4.26−4.31 (m, 3H), 4.37−4.41 (m, 2H), 5.25−5.27 (m, 1H), 5.79 (d, J = 7.4 Hz, 1H), 6.18−6.25 (m, 1H), 6.36−6.42 (m, 3H), 7.43−7.45 (m, 2H), 7.64 (d, J = 7.5 Hz, 1H), 8.21−8.24 (m, 2H). ^{13}C NMR ($CDCl_3$, 100 MHz): 25.8, 28.3, 28.7, 28.8, 35.5, 36.9, 38.7, 55.4, 56.1, 59.8, 61.7, 65.8, 73.5, 82.0, 95.7, 101.2, 108.1, 109.0, 116.4, 116.8, 118.9, 119.5, 121.7, 124.7, 126.9, 127.0, 128.1, 130.5, 140.7, 142.1, 147.7, 153.7, 155.6, 163.3, 163.4, 166.3, 172.5 ppm. ESI-MS: calcd for $C_{37}H_{42}F_2N_9O_{13}S_3$(M+1), 954.20; found, 954.21.

Synthesis of 6. To a MeOH (3.0 mL) solution of **1** (200 mg, 0.98 mmol), **9** (277 mg, 0.98 mmol) and sodium ascorbate (10 mol %) were added. The reaction mixture as degassed for 15 min by purging argon gas. Then 5 mol % of $CuSO_4$ in 0.5 mL water was added to the reaction mixture and stirred for 4 h. Then the crude reaction mixture was directly passed through silica column chromatography using DCM/MeOH (8.5:1.5) as eluent to afford a yellow solid **9** (270 mg, 57% yield). ^{1}H NMR (400 MHz, DMSO-d_6): δ 1.21−1.30 (m, 2H), 1.39−1.56 (m, 4H), 2.08 (t, J = 6.7 Hz, 2H), 2.51 (br s, 1H), 2.74−2.78 (m, 1H), 3.03−3.07 (m, 2H), 4.07−4.10 (m, 1H), 4.25−4.27 (m, 1H), 6.32 (s, 1H), 6.39 (s, 1H), 6.81 (br s, 1H), 6.87 (d, J = 6.3 Hz, 1H), 7.71 (d, J = 7.8 Hz, 1H), 8.32 (br s, 1H), 8.37−8.39 (m, 1H), 8.54 (br s, 1H). ^{13}C NMR ($CDCl_3$, 100 MHz): 25.9, 28.7, 28.9, 34.6, 35.7, 39.7, 56.1, 59.9, 61.7, 102.8, 111.0, 115.0, 120.0, 124.3, 131.6, 136.7, 146.1, 155.3, 157.0, 163.2, 163.4, 172.8 ppm. HRMS: calcd for $C_{22}H_{25}N_6O_5S$ (M+1), 485.1607; found, 485.1606.

Synthetic Materials and Methods. Chemicals used in this project were purchased from Aldrich, Alfa-Aesar, Carbosynth, TCI, and Ducsan without further purification. Silica gel 60 (Merck, 0.063−0.2 mm) was used for column chromatography. Analytical TLC was performed using Merck 60 F254 silica gel (precoated sheets, 0.25 mm thick). ^{1}H and ^{13}C NMR spectra were collected in $CDCl_3$, DMSO (Cambridge Isotope Laboratories, Cambridge, MA) on Varian 300 and 400 MHz spectrometers. All chemical shifts are reported in ppm value using the peak of residual proton signals of TMS as an internal reference. The mass spectra were obtained on an Ion Spec HiRes mass spectrometer.

Spectroscopic Materials and Methods. Stock solutions of biologically relevant analytes [thiols, Val, Tyr, Thr, Tau, Ser, Pro, Phe, Met, Lys, Leu, Ile, His, Gly, Gluc, Glu, Gln, Asp, Asn, Arg, Ala, Trp, Zn(II), Na(I), Mg(II), K(I), Fe(III), Fe(II), Cu(II) and Ca(II)] were prepared in triple-distilled water. Stock solutions of **5** were also prepared in triple-distilled water. All spectroscopic measurements were performed under physiological conditions (PBS buffer containing 25% (v/v) of DMSO, pH 7.4, 37 °C). Absorption spectra were recorded on a S-3100 (Scinco) spectrophotometer, and fluorescence spectra were recorded using an RF-5301 PC spectrofluorometer (Shimadzu) equipped with a xenon lamp. Samples for absorption and emission measurements were contained in quartz cuvettes (3 mL volume). Excitation was provided at 410 nm with excitation and emission slit widths of 3 and 3 nm, respectively.

Preparation of Cell Cultures. Human lung adenocarcinoma epithelial cells (KCLB, Seoul, Korea) were cultured in RPMI (WelGene Inc., Seoul, Korea) supplemented with 10% FBS (WelGene), penicillin (100 units/ml), and streptomycin (100 μg/mL). Two days before imaging, the cells were passed and plated on glass-bottomed dishes (MatTek). All the cells were maintained in a humidified atmosphere of 5/95 (v/v) of CO_2/air at 37 °C. For labeling, the growth medium was removed and replaced with RPMI without FBS. The cells were treated and incubated with ligand at 37 °C under 5% CO_2 for 15 min. The cells were washed three times with phosphate buffered saline (PBS; Gibco) and then imaged after further incubation in colorless serum-free media for 15 min.The cells were seeded on 24-well plates and stabilized for overnight. Compound **5** was applied to the cells to monitor their uptake and drug release, as discussed in the main text above. In some experiments, the cells were incubated with media containing lyso- or ERtracker prior to treatment with **5**. Then the cells were briefly washed with 1 mL of PBS and were then treated with **5** in PBS. After incubation, residual quantities of **5** that were not taken up in the cells were removed by washing the cells three times with PBS before the cells were placed in 1 mL of a PBS solution. Fluorescence images were taken using a confocal laser scanning microscope (Zeiss LSM 510, Zeiss, Oberko, Germany).

■ ASSOCIATED CONTENT

Supporting Information

Additional spectra (UV−vis absorption, fluorescence, NMR, ESI-MS, HRMS) and cell viability data. This material is available free of charge via the Internet at http://pubs.acs.org.

■ AUTHOR INFORMATION

Corresponding Author

kangch@khu.ac.kr; jongskim@korea.ac.kr

Notes

The authors declare no competing financial interest.

■ ACKNOWLEDGMENTS

This work was supported by the CRI project (20120000243) (J.S.K.) and by Basic Science Research Program (2012R1A1A2006259) (C.K.) through the National Research Foundation of Korea funded by Ministry of Education, Science and Technology

■ REFERENCES

(1) (a) Garnett, M. C. *Adv. Drug Delivery Rev.* **2001**, *53*, 171−216. (b) Jaracz, S.; Chen, J.; Kuznetsova, L. V.; Ojima, I. *Bioorg. Med. Chem.* **2005**, *13*, 5043−5054. (c) Yokoyama, M. *J. Artif. Organs* **2005**, *8*, 77−84. (d) Torchilin, V. P.; Schafer-Korting, M. *Handbook of Experimental Pharmacology*; Springer: Berlin, 2010; p 3.

(2) Andersen, E. S.; Dong, M.; Nielsen, M. M.; Jahn, K.; Subramani, R.; Mamdouh, W.; Golas, M. M.; Sander, B.; Stark, H.; Oliveira, C. L. P.; Pedersen, J. S.; Birkedal, V.; Besenbacher, F.; Gothelf, K. V.; Kjems, J. *Nature* **2009**, *459*, 73−76.

(3) (a) Brown, S. D.; Nativo, P.; Smith, J.-A.; Stirling, D.; Edwards, P. R.; Venugopal, B.; Flint, D. J.; Plumb, J. A.; Graham, D.; Wheate, N. J. *J. Am. Chem. Soc.* **2010**, *132*, 4678−4684. (b) Voliani, V.; Signore, G.;

Nifosí, R.; Ricci, F.; Luin, S.; Beltram, F. *Recent Pat. Nanomed.* **2012**, *2*, 1−11.
(4) Jung, J.; Solanki, A.; Memoli, K. A.; Kamei, K.-I.; Kim, H.; Drahl, M. A.; Williams, L. J.; Tseng, H.-R.; Lee, K. *Angew. Chem., Int. Ed.* **2010**, *122*, 107−111.
(5) Francis, M. F.; Cristea, M.; Winnik, F. M. *Pure Appl. Chem.* **2004**, *76*, 1321−1335.
(6) (a) Yang, P.; Gai, S.; Lin, J. *Chem. Soc. Rev.* **2012**, *41*, 3679−3698. (b) Singh, N.; Karambelkar, A.; Gu, L.; Lin, K.; Miller, J. S.; Chen, C. S.; Sailor, M. J.; Bhatia, S. N. *J. Am. Chem. Soc.* **2011**, *133*, 19582−19585.
(7) Lee, M. H.; Kim, J. Y.; Han, J. H.; Bhuniya, S.; Sessler, J. L.; Kang, C.; Kim, J. S. *J. Am. Chem. Soc.* **2012**, *134*, 12668−12674.
(8) Plunkett, W.; Huang, P.; Gandhi, V. *Anti-Cancer Drugs* **1995**, *6*, 7−13.
(9) Noble, S.; Goa, K. L. *Drugs* **1997**, *54*, 447−472.
(10) Friberg, G.; Kindler, H. *Curr. Oncol. Rep.* **2005**, *7*, 186−195.
(11) Zhang, J.; Visser, F.; King, K.; Baldwin, S.; Young, J.; Cass, C. *Cancer Metastasis Rev.* **2007**, *26*, 85−110.
(12) Reid, J. M.; Qu, W.; Safgren, S. L.; Ames, M. M.; Krailo, M. D.; Seibel, N. L.; Kuttesch, J.; Holcenberg, J. *J. Clin. Oncol.* **2004**, *22*, 2445−2451.
(13) Moog, R.; Burger, A.; Brandl, M.; Schuler, J.; Schubert, R.; Unger, C.; Fiebig, H.; Massing, U. *Cancer Chemother. Pharmacol.* **2002**, *49*, 356−366.
(14) Chen, S.; Zhao, X.; Chen, J.; Chen, J.; Kuznetsova, L.; Wong, S. S.; Ojima, I. *Bioconjug. Chem.* **2010**, *21*, 979−987.
(15) Sivakumar, K.; Xie, F.; Cash, B. M.; Long, S.; Barnhill, H. N.; Wang, Q. *Org. Lett.* **2004**, *6*, 4603−4606.
(16) Cordero, F. M.; Bonanno, P.; Chioccioli, M.; Gratteri, P.; Robina, I.; Vargas, A. J. M.; Brandi, A. *Tetrahedron* **2011**, *67*, 9555−9564.
(17) Kim, H. -C.; Kreiling, S.; Greiner, A.; Hampp, N. *Chem. Phys. Lett.* **2003**, *372*, 899−903.
(18) Gregory, J. D. *J. Am. Chem. Soc.* **1955**, *77*, 3922−3923.
(19) Cerqueira, N. M. F. S. A.; Fernandes, P. A.; Ramos, M. J. *Chem.—Eur. J.* **2007**, *13*, 8507−8515.
(20) Heo, D. N.; Yang, D. H.; Moon, H. -J.; Lee, J. B.; Bae, M. S.; Lee, S. C.; Lee, W. J.; Sun, I. -C.; Kwon, I. K. *Biomaterials* **2012**, *33*, 856−866.